Biosensors and Bioelectronics 24 (2008) 272–278

Contents lists available at ScienceDirect

Biosensors and Bioelectronics

journal homepage: www.elsevier.com/locate/bios

Increasing amperometric biosensor sensitivity by length fractionated single-walled carbon nanotubes

Federico Tasca[a,*], Lo Gorton[a], Jakob B. Wagner[b], Gilbert Nöll[a,*]

[a] Department of Analytical Chemistry, Lund University, P.O. Box 124, SE-221 00 Lund, Sweden
[b] Polymer and Material Chemistry, nCHREM, Lund University, P.O. Box 124, SE-221 00 Lund, Sweden

ARTICLE INFO

Article history:
Received 21 December 2007
Received in revised form 28 March 2008
Accepted 31 March 2008
Available online 6 April 2008

Keywords:
Amperometric biosensor
Diaphorase
NADH oxidation
Osmium redox polymer hydrogel
Length-separated single-walled carbon nanotubes (SWCNTs)
Transmission electron microscopy (TEM)

ABSTRACT

In this work the sensitivity-increasing effect of single-walled carbon nanotubes (SWCNTs) in amperometric biosensors, depending on their average length distribution, was studied. For this purpose the SWCNTs were oxidatively shortened and subsequently length separated by size exclusion chromatography. Transmission electron micrographs of different fractions of SWCNTs were collected. Diaphorase "wired" to an osmium redox polymer was blended with the shortened SWCNTs of different lengths. Depending on the average length of the SWCNTs the sensitivity of the amperometric biosensor model system towards oxidation of 1,4-dihydronicotinamide adenine dinucleotide (NADH) was increased by a factor of five. The best performance was achieved with SWCNTs of medium length. The linear range for NADH detection was between 5 μM and 7 mM, the maximum sensitivity was 47 nA μM^{-1} cm^{-2}, and the detection limit was 1 μM. The biosensor exhibited excellent electrocatalytic properties. Even at relatively high NADH concentrations the oxidative current was limited by the diffusion rate of NADH.

1. Introduction

In recent years, the sensitivity of amperometric biosensors has been enhanced by incorporating carbon-based materials in these devices (Balavoine et al., 1999; Binyamin et al., 2000; Joshi et al., 2005). Among these materials carbon nanotubes were the most effective (Granot et al., 2006; Joshi et al., 2005; Lawrence et al., 2005; Liu et al., 2005, 2007; Luo et al., 2006; Rivas et al., 2007; Rubianes and Rivas, 2005; Timur et al., 2007; Tu et al., 2005, 2007; Wang, 2005; Zhang et al., 2007). Since their discovery in 1991 (Iijima, 1991), their manufacturing procedures were improved and nowadays carbon nanotubes can be purchased from different suppliers at a reasonable price. With easier accessibility research on the utilization of carbon nanotubes for electronic and analytical purposes increased dramatically. In particular, single-walled carbon nanotubes (SWCNTs) are of strong interest due to their large surface to volume ratio, and their unique electrical, chemical, and mechanical properties (Britz and Khlobystov, 2006; Ericson et al., 2004; Fagan et al., 2007; Gooding and Shapter, 2005; Messersmith and Textor, 2007; Ziegler, 2005). For applications in amperometric biosensors carbon nanotubes have been employed since 2002 (Musameh et al., 2002; Xue et al., 2002). Different strategies for immobilizing carbon nanotubes on an electrode have been reported, such as carbon nanotube paste electrodes prepared by mixing carbon nanotubes and mineral oil (Antiochia and Gorton, 2007; Rivas et al., 2007; Rubianes and Rivas, 2005; Valentini et al., 2004), in situ electropolymerization in the presence of carbon nanotubes (Callegari et al., 2004; Granot et al., 2006; Ma et al., 2006), deposition of carbon nanotubes on glassy carbon electrodes in association with Nafion (Choi et al., 2007; Lee et al., 2007; Li et al., 2007; Liu and Cai, 2007; O'Connor et al., 2004; Wang et al., 2003), or incorporation of carbon nanotubes into redox polymer hydrogels (Joshi et al., 2005; Wang et al., 2006). Most frequently the SWCNTs have been used without length separation. There might be large differences in quality, morphology, and length of the applied SWCNTs which can have strong influence on the performance of the resulting biosensors. Very often transition metal particles are required during the nanotube manufacturing process and they might still be present in the nanotubes after purification. In fact, some of the electrocatalytical properties, which have been claimed for multi-walled carbon nanotubes, were caused by transition metal impurities (Banks et al., 2006; Sljukic et al., 2006).

In this contribution we compare the performance of SWCNTs of different lengths for applications in amperometric biosensors. This will be achieved by using SWCNTs obtained from three different suppliers (a) ABCR, Karlsruhe, Germany, (b) Sigma–Aldrich (http://www.sigmaaldrich.com), purity 50–70%, and (c) Nanocyl,

* Corresponding author.
E-mail addresses: Federico.tasca@analykem.lu.se (F. Tasca), Gilbert.Noll@analykem.lu.se (G. Nöll).

0956-5663/$ – see front matter © 2008 Elsevier B.V. All rights reserved.
doi:10.1016/j.bios.2008.03.038

Sambreville, Belgium. They were classified by transmission electron microscopy (TEM), and examined for their efficiency in a biosensor prototype after immobilization into a redox polymer hydrogel. Large differences were obtained in terms of sensitivity, i.e. oxidation current for 1,4-dihydronicotinamide adenine dinucleotide (NADH) when they were employed in a diaphorase (DI) based biosensor. Next the nanotubes of highest quality were oxidatively shortened followed by a chromatographic separation of the nanotubes with respect to their length. A detailed shortening length-separation protocol is reported. The effect of the length distribution on the biosensing response was studied for each fraction and TEM images of individual fractions of the shortened nanotubes were obtained.

We have chosen DI "wired" to the osmium redox polymer poly(vinylpyridine)-[osmium-(*N*,*N*′-methylated-[2,2′]-biimidalzole)$_3$]$^{2+/3+}$ ($E^{0'} \approx 90$ vs. the normal hydrogen electrode, NHE) (Heller, 2004) as a bioelectrocatalytic system, which could be easily blended with the SWCNTs. Poly(ethylene glycol) diglycidyl ether (PEGDGE) was used as a cross-linker (Ohara et al., 1993). DI is "wired" by the redox polymer and catalyzes the oxidation of NADH to NAD$^+$ (Antiochia and Gorton, 2007). The electrons gained from oxidation of NADH by DI are transferred from DI to the Os polymer and from there further to the electrode. For this process a potential keeping the Os polymer in its oxidized form has to be applied (for thermodynamic reasons the redox potential of the Os polymer has to be slightly more positive than the redox potential of DI). Direct oxidation of NADH at unmodified electrodes requires a large overpotential (>1 V), due to slow electron transfer kinetics and electrode fouling by adsorption of oxidation products (Bardea et al., 1997; Barton et al., 2004; Gorton and Domínguez, 2002). Various methodologies have been developed to facilitate the NADH electron transfer kinetics (Bardea et al., 1997; Gorton and Domínguez, 2002). DI "wired" to an electrode can be applied in combination with NAD$^+$-dependent dehydrogenases, which catalyze the oxidation of specific substrates with concomitant NAD$^+$-reduction (Antiochia and Gorton, 2007; Gorton and Domínguez, 2002). NAD$^+$/NADH-dependent dehydrogenases constitute the largest group of redox enzymes known today (Antiochia and Gorton, 2007; Bullen et al., 2006; Gorton and Domínguez, 2002). In combination with NADH:quinone oxidoreductases (NQOs) such as DI, a large variety of biosensors based on NADH redox cycling can be developed. NAD$^+$/NADH is biologically active in a diffusional route and, similar to the substrate, the soluble NAD$^+$/NADH is associated with the protein only during the catalytic event. Since biosensors based on NAD$^+$/NADH redox cycling have to be cheap and are developed for fast and single use, their limitation due to diffusion of NADH is not an obstacle.

2. Experimental

2.1. Chemicals and materials

DI (E.C. 1.6.99.-) from *Bacillus stearothermophilus* (Unitika LTD., JP Bldg., 3-4-4 Nihonbashi-Muromachi, Chuo-ku, Tokyo, Japan 103-8321) was generously donated by Dr. E. Burestedt, HemoCue, Ängelholm, Sweden. The enzyme activity determined through enzyme assay (Mains et al., 1980) was 960 U/mg protein. NADH was obtained from Sigma (St. Louis, MO, USA) as lyophilized powder, and solutions were prepared daily by dissolving the appropriate amounts in the carrier buffer. Water was purified in a Milli-Q water purification system (Millipore, Bedford, MA, USA). PEGDGE was obtained from Polysciences (Warrington, PA, USA). Poly(vinylpyridine)-[osmium-(*N*,*N*′-methylated-2,2′-biimidalzole)$_3$]$^{2+/3+}$ ($E^{0'} \approx 90$ mV vs. NHE) was synthesized as reported elsewhere (Mao et al., 2003). SWCNTs from three different suppliers were applied: (a) ABCR, Karlsruhe, Germany (b) Sigma–Aldrich (http://www.sigmaaldrich.com), purity: 50–70% (c) Nanocyl, Sambreville, Belgium. Triton X-100 and controlled pore glass (CPG 3000 Å) were both from Fluka (Buchs, Switzerland). Spectrographic graphite electrodes were from Ringsdorff Werke GmbH, Bonn, Germany (type RW001, 3.05 mm diameter and 13% porosity http://www.sglcarbon.com/). All solutions used for immobilization were prepared in Milli-Q water, and the NADH used as substrate was dissolved in bis–tris, or phosphate, or tris 0.1 M working buffer solutions depending on the pH. The working buffer solutions were degassed before use to avoid air bubbles in the flow system.

2.2. Electrode preparation and equipment

Flow injection measurements were performed with a flow-through amperometric cell of the wall-jet type (Appelqvist et al., 1985) at an applied potential of +290 mV vs. NHE. The carrier flow was maintained at a constant flow rate of 1 ml min^{-1} by a peristaltic pump. The injection loop volume was 50 μl. The dispersion factor (Ruzicka and Hansen, 1988) of the system was 1.04 at this flow rate. Cyclic voltammetry was performed using an Autolab PGSTAT30 (Eco Chemie, Utrecht, Netherlands) electrochemical potentiostat/galvanostat. A three-electrode cell consisting of modified electrodes (described below) as working electrodes, a saturated calomel reference electrode (SCE), and a platinum foil counter electrode was used. High resolution TEM images were acquired on a JEOL 3000F field emission TEM at 300 kV (JEOL, Tokyo, Japan), with a 2k × 2k ultrascan CCD camera (Gatan, Warrendal, PA, USA). The microscope has a point resolution of 0.165 nm in TEM mode.

Graphite electrodes were polished as reported previously (Tasca et al., 2007). In this work, 0.7 mg of each of the three different SWCNT preparations (a), (b), and (c) were dissolved in 1 ml of Milli-Q water through overnight sonication. Then 5 μl of dispersion (a), or (b), or (c) were placed on the top of the polished electrode and spread evenly using a microsyringe tip. Next, 2 μl of the osmium redox polymer (10 mg/ml in Milli-Q water) were mixed to the 5 μl of SWCNT solution. Following this, 5 μl of enzyme (0.1 mg/ml in Milli-Q water) was added to the mixture. Finally 1 μl of PEGDGE (1 mg/ml) was added. The electrode was then allowed to dry and placed overnight at 4 °C for complete cross-linking reaction. Electrodes not including SWCNTs were prepared as described above but without any of the SWCNT dispersions. The amounts of SWCNTs, redox polymer, PEGDGE and DI chosen in this work are in accordance with previous reports (Antiochia and Gorton, 2007; Binyamin et al., 2000; Joshi et al., 2005; Tasca et al., 2007).

2.3. Oxidative shortening and length separation of the SWCNTs

In order to perform the oxidative shortening, a suspension of 200 mg of SWCNTs and a mixture of 6 ml of sulfuric acid and 2 ml of nitric acid (98% and 70%, respectively) was sonicated for 6 h at 40 °C. The solution was then adjusted to pH 7 by adding a solution of NaOH. Thereafter the solvent was removed by centrifugation. The SWCNTs were then dissolved in a 1 wt% Triton X-100 Milli-Q water solution, and stabilized by sonication over night. The dispersion was length separated by flash chromatography using a column filled with controlled pore glass (CPG 3000 Å). Milli-Q water was used as eluent. Nine fractions of equal volume containing SWCNTs were collected. Following this procedure the total yield of shortened SWCNTs was about 10%. The yield could be further increased by adding Triton X-100 also in the eluent during chromatography. But in that case the concentration of surfactant in the resulting nanotube suspensions was too high for proper electrode preparation.

3. Results and discussion

Our intension was to compare the performance of SWCNTs of different lengths for applications in amperometric biosensors. Since the yield of SWCNTs after an oxidative shortening process by addition of strong acids followed by chromatography is expected to be rather low (about 10%), we first investigated unmodified SWCNTs of three different suppliers. These investigations were performed in order to find the best start material that gives the highest electrocatalytic current and to compare the electrocatalytic properties of the SWCNTs before and after oxidative shortening. For flow injection analysis (FIA) each SWCNT/DI/Os polymer coated electrode was placed in a flow through electrochemical cell and examined in the flow injection mode. A constant potential of +290 mV vs. NHE was applied and the NADH oxidation current was measured at different concentrations of NADH, which was then used to quantify the sensitivity-increasing effect of SWCNTs. At the applied potential the redox polymer is completely in its oxidized state and the electron transfer from the active site of DI to the redox polymer is favored. Calibration curves for NADH oxidation for the different DI-redox polymer electrodes are shown in Fig. 1A. For all electrodes the linear range for NADH detection was between concentrations of 5 μM and 7 mM. In Fig. 1B the oxidation currents (as average of three-independent measurements) detected after injection of a 1 mM NADH solution are depicted. When the DI containing redox polymer hydrogels were blended with unmodified SWCNTs, the current detected for NADH oxidation was increased by a factor of 2.5, which is in agreement with previously reported investigations of the sensitivity-increasing effect of SWCNTs in amperometric biosensors (Antiochia and Gorton, 2007; Joshi et al., 2005). When SWCNTs were modified with glucose oxidase and then incorporated in an osmium redox polymer hydrogel the sensitivity for glucose sensing was increased by a factor of 3 (Joshi et al., 2005). Interestingly, we found a significant difference in the performance of the SWCNTs depending on their origin. With respect to the oxidation current obtained in the absence of any SWCNTs, only a 1.3-fold increase was obtained by blending the DI-redox polymer hydrogel with SWCNTs from supplier (a), whereas the sensitivity was increased by a factor of 2 and 2.5 with SWCNTs from supplier (b) and (c), respectively (at a NADH concentration of 1 mM, see Fig. 1B).

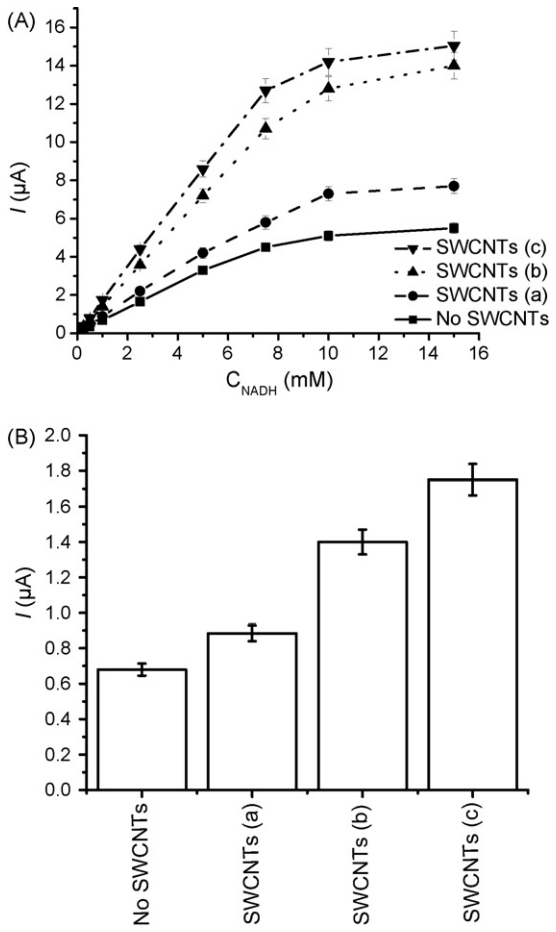

Fig. 1. Effect of blending the DI-redox polymer electrodes with SWCNTs. (A) NADH calibration curves for DI-redox polymer electrodes without SWNTs (■), and blended with SWCNTs from supplier (a) (●), (b) (▲), (c) (▼). (B) Oxidation peak currents during FIA by injection of 1 mM NADH solution.

In order to elucidate the reason for this different behavior, we performed high-resolution transmission electron microscopy (TEM) investigations of the SWCNTs. In Fig. 2A, B, B′, and C, representative TEM images of the different samples of SWCNTs are depicted. Notably, the vast majority of CNTs in the samples was observed to be single-walled. As is obvious in Fig. 2A, in the sample of supplier (a) only a very low fraction of SWCNTs was present besides a large amount of amorphous carbon and catalyst particles. The sample of supplier (b), shown in Fig. 2B, exhibited a significantly higher quantity. A high number of very long SWCNTs was found. Nevertheless, a large amount of transition metal catalyst particles (represented by the darker spheres in the figure) was present as well. From Fig. 2B′, representing a higher magnification of sample (b), it can be observed that the growth of several SWCNTs was catalyzed by the same particle. The sample of supplier (c) depicted in Fig. 2C contained almost pure SWCNTs of high quantity. Since the DI-redox polymer hydrogel blended with SWCNTs from supplier (c) exhibited the highest current for NADH oxidation, it is obvious that the sensitivity-increasing effect was caused by the SWCNTs and not by the addition of transition metal particles.

Next we decided to determine the effect of the length distribution of the carbon nanotubes on their sensitivity-increasing effect with respect to NADH determination (oxidation). For this purpose SWCNTs of supplier (c) were oxidatively shortened by acid treatment and subsequently purified and length separated by size exclusion chromatography according to Patolsky et al. (2004). Nine fractions of equal volume containing SWCNTs were collected. By this separation method the average length of the SWCNTs decreased from fraction 1 to 9. Experimental details are described in Section 2.

For FIA experiments 1 ml of each fraction was lyophilized in order to calculate the concentration of SWCNTs. Milli-Q water was added to each fraction until a final concentration of 0.7 mg ml^{-1} was achieved. Electrodes were prepared as described previously and blended with the shortened SWCNTs of different lengths. Three electrodes immobilized with each of the 9 fractions were investigated with FIA. In Fig. 3 the oxidative current detected after injection of a 1 mM solution of NADH is depicted for the DI-redox polymer electrodes blended with the 9 different fractions of SWCNTs. The highest NADH oxidation current was detected in fraction 4 and 5. A sensitivity of 47 nA μM^{-1} cm^{-2} and a detection limit of 1 μM were determined. This detection limit for NADH is five times lower than that estimated at a DI/Os polymer/carbon nanotube paste electrode which was recently published (Antiochia and Gorton, 2007). Furthermore, our system exhibits a larger linear dynamic range, a higher sensitivity, and is working at a less positive potential.

When the DI containing redox polymer hydrogels were blended with fractions 4 and 5, the current was increased almost by a factor of two compared to the response of the hydrogel blended with the non-treated SWCNTs (see Figs. 1B and 3). Compared to

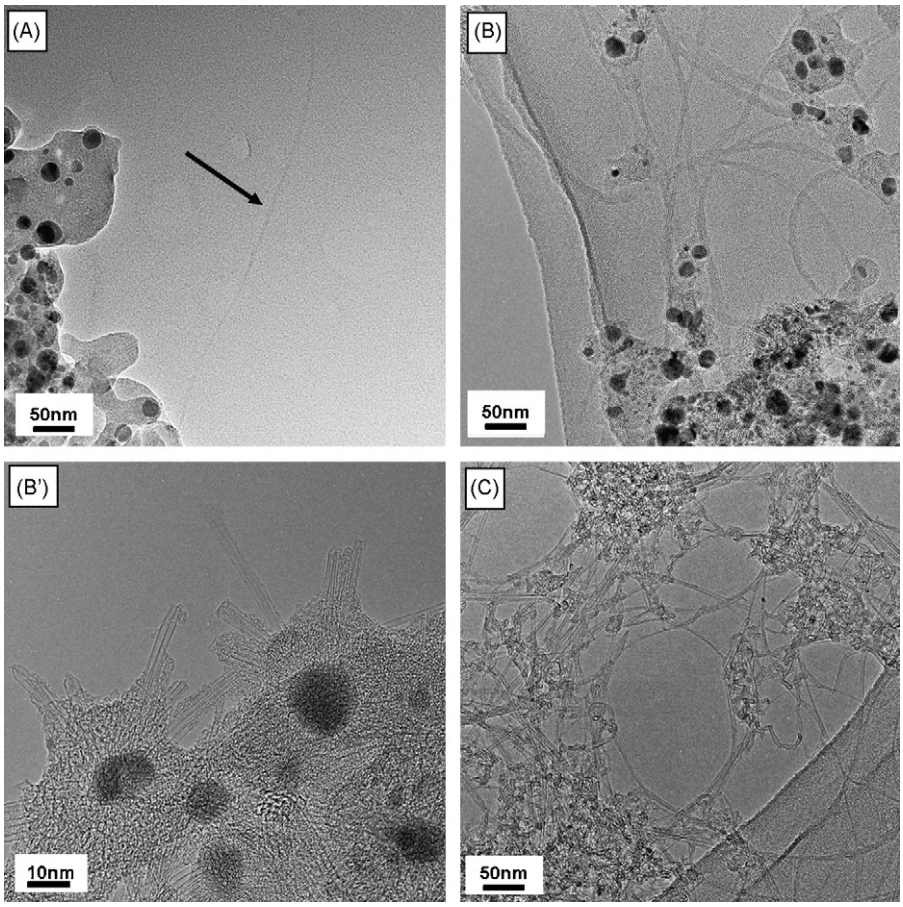

Fig. 2. Representative high resolution TEM images of SWCNTs from three different suppliers dispersed in water. (A) Image of a sample from supplier (a). Only few SWCNTs are present under the amorphous carbon on the left corner of the image and an isolated nanotube is indicated by an arrow. (B) Image of a sample from supplier (b). Many transition metal catalyst particles are present beside the SWCNTs. (B′) Higher magnification of the sample from supplier (b). The growth of CNTs starting at the catalyst particles can be seen. (C) Image of a sample from supplier (c). SWCNTs of different shape are present at high purity.

the response of the hydrogels without SWCNTs the current was increased by a factor of five. The higher sensitivity obtained with the shortened SWCNTs can be explained by the removal of catalyst particles, amorphous graphite, and impurities in general. Interestingly, the detected sensitivity has a maximum for SWCNTs of medium length. For very short nanotubes it is expected that most of the DI redox centers can be accessed (because the blending should be most effective), whereas rather long nanotubes would enhance the charge transport over large distances, e.g. from the outer part of the hydrogel to the electrode. Obviously there exists a certain length distribution, which allows the optimization of both parameters. This optimum length is expected to vary for different redox enzymes embedded in redox polymers. It has been speculated that SWCNTs can partially unfold some redox enzymes and thereby increase the electrocatalytic current because the electroactive site of the enzyme becomes more easily accessible (Joshi et al., 2005; Liu et al., 2004; Zhao et al., 2002). In our case, it is unlikely that partial unfolding of the enzyme had resulted in an increase in the oxidation current because the unfolding should be most effective when the shortest SWCNTs are used.

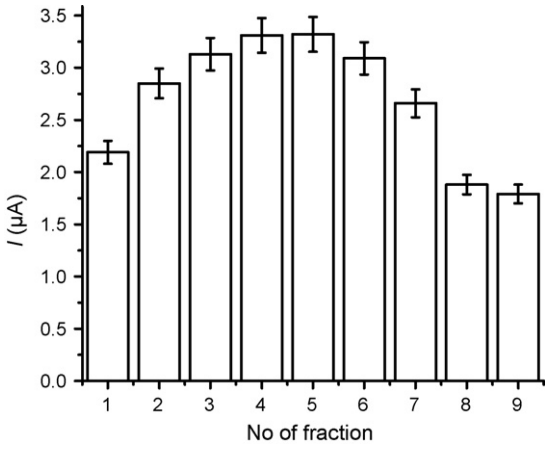

Fig. 3. Response of DI-redox polymer modified electrodes blended with nine fractions of SWCNTs of different length (1: longest, 9: shortest) after injection of 1 mM NADH.

Control experiments were performed with DI adsorbed at a graphite electrode in the presence of SWCNTs but without any redox polymer. In these experiments, we could not detect a significant amount of electrocatalytic current for NADH oxidation. When the redox polymer hydrogel was prepared with SWCNTs but without DI, no electrocatalytic current could be detected either. It has been reported that SWCNTs adsorbed on electrodes reduce the overpotential for NADH oxidation (Choi et al., 2007; Liu and Cai, 2007). Furthermore the oxidative treatment of SWCNTs with sulfuric and nitric acid may lead to the introduction of nitro groups (Forrest and Alexander, 2007), and nitrocompounds immobilized on nanostructured electrodes have been shown to catalyze the oxidation of NADH at small overpotentials (De Leo et al., 2007; Mano

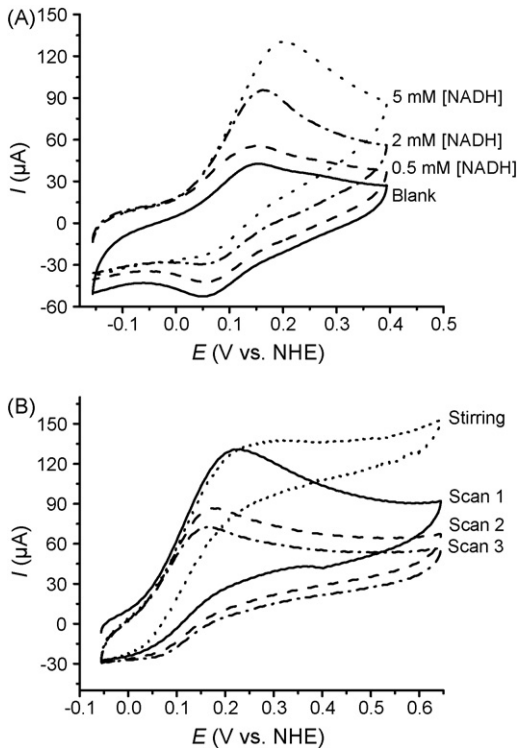

Fig. 4. (A) CVs of a DI-redox polymer modified electrode blended with SWCNTs from fraction 5 at increased concentrations of NADH (scan rate: 50 mV s^{-1}). (B) Multi-cycle CV (three cycles) of a similar electrode in a solution of NADH of a concentration of 5 mM. A CV collected during stirring of the solution (dotted curve) is depicted as well.

and Kuhn, 2001; Mano et al., 2001). However, at the potential we applied during FIA (+290 mV vs. NHE) we did not detect any electrocatalytic current in the absence of DI, i.e. the NADH oxidation was not catalyzed directly by the SWCNTs or the osmium redox polymer.

In Fig. 4A cyclic voltammograms (CVs) of a DI-redox polymer modified electrode blended with SWCNTs from fraction 5 at increasing concentrations of NADH are shown. The bioelectrocatalytic oxidation of NADH was observed at $E > +150$ mV vs. NHE and the electrocatalytic anodic current increased with concentrations of NADH. Even at an NADH concentration of 5 mM the anodic current reached a well-defined peak maximum. After the maximum was reached the current decreased. We also measured the oxidation of NADH at a concentration of 10 mM at different scan rates (10–350 mV s^{-1}, data not shown). The current at the peak maxima was proportional to the square root of the scan rate indicating that the electrocatalytic current was limited by diffusion of NADH, but not by the catalytic turnover of DI or the charge transfer rate within the hydrogel, i.e. the DI-redox polymer hydrogel blended with SWCNTs was highly efficient. This conclusion is also supported by multi-cycle CVs shown in Fig. 4B. The anodic peak current decreased with each cycle due to the depletion of NADH from the diffusion layer. If the solution was stirred during the CV experiment, the anodic current remained at its highest value after the maximum was reached (see dotted CV curve in Fig. 4B). This behavior can be explained by an increased mass transport.

In order to characterize the shape and the degree of purity of the shortened SWCNTs in the different fractions TEM investigations were performed. In Fig. 5 representative images of fraction 5 (Fig. 5A), 7 (Fig. 5B), and 9 (Fig. 5C) are presented. As it can be concluded from these images fraction 5 and 7 still consisted of relatively long SWCNTs. The purity of the SWCNTs was very high.

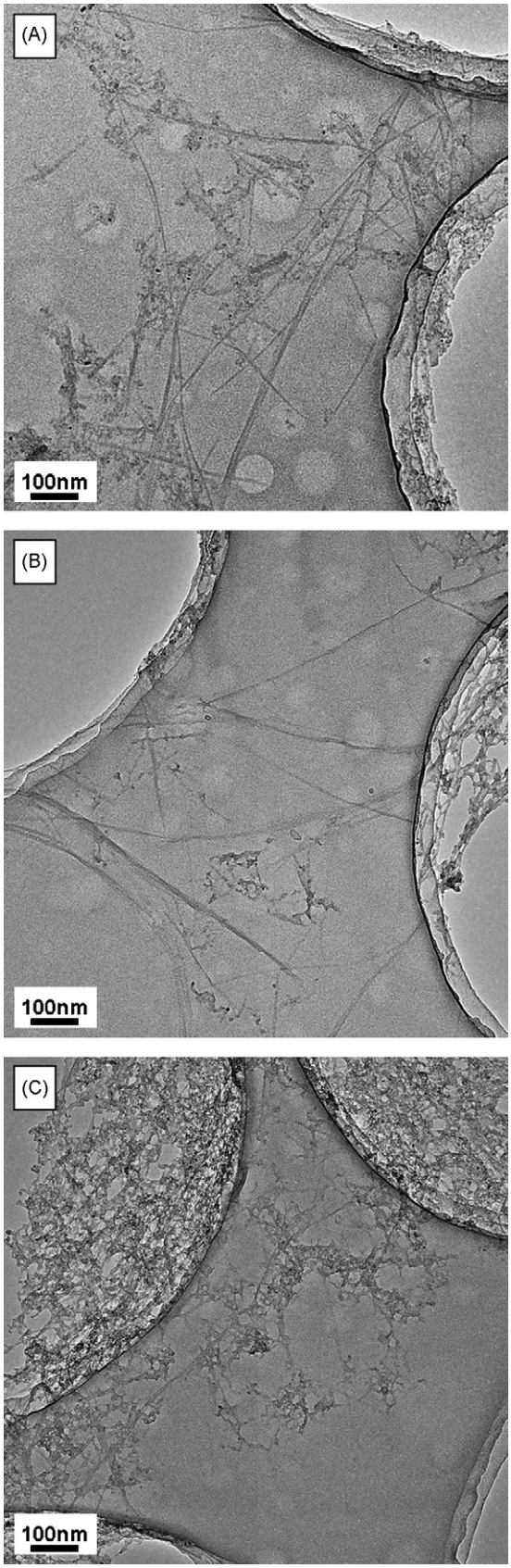

Fig. 5. Representative high-resolution TEM images of shortened SWCNTs. (A) Image of fraction 5. This fraction contains still relatively long SWCNTs. (B) Image of fraction 7. (C) Image of fraction 9. This fraction contains the shortest SWCNTs.

Almost no transition metal particles could be detected. Also no significant amount of amorphous graphite seemed to be present. From Fig. 5C it is obvious that the SWCNTs in fraction 9 were the shortest. In a recent publication SWCNTs (purchased from HiPco. CNI, Houston TX) were oxidatively shortened and analyzed by TEM (Forrest and Alexander, 2007). The authors reported that oxidative shortening for 6 h resulted in SWCNTs with an average length of 94 nm and that the individual nanotubes were between 25 nm and 225 nm in length. The largest decrease in length during oxidative shortening was observed during the first 6 h (unshortened SWCNTs had an average length of 650 nm, the average length was decreased to 94 nm after 6 h, and to 67 nm after 12 h of oxidative shortening). Assuming that oxidative shortening of the SWCNTs applied in this work results in a similar length distribution, the chromatographic separation should result even in a narrower length distribution of the individual fractions. After deposition of the SWCNTs on the carbon coated TEM sample grids the solvent had to evaporate. During this process the SWCNTs started to agglomerate. They tended to stick together along their longitudinal axes resulting in the formation of bundles. Therefore, a quantitative determination of the average length of the SWCNTs present in the distinct fractions was not possible. A few separated SWCNTs were found as well but their individual length was not regarded to be representative for an entire fraction. In preliminary results on applying the length-separated nanotubes together with two other redox enzymes, the electrocatalytic current could also be increased. Depending on the enzyme either fraction 1 or fraction 8 gave best results. Consequently there is no specific length distribution which shows optimum electrocatalytic performance in general. Instead, the average length of the SWCNTs has to be optimized individually for each type of redox enzyme.

When SWCNTs are treated with strong oxidative acids (e.g. to remove impurities such as transition metal particles), this may result not only in shorter SWCNTs, which contain additional carboxy functionalities, but also in more serious damage to the SWCNTs leading to the presence of additional impurities. When we performed the size exclusion chromatography the yield of shortened SWCNTs was rather low. The majority of the carbon material remained permanently adsorbed at the top of the column. This material might consist of SWCNTs which are still rather long, SWCNTs present in large bundles, or impurities. Therefore, we believe that after acid treatment further purification steps such as chromatography have to follow before pure shortened SWCNTs can be obtained.

4. Conclusions

DI was used as a model enzyme “wired” to an osmium redox polymer hydrogel on the surface of graphite electrodes for the detection of NADH in a linear range from 5 μM to 7 mM with a limit of detection (3 S.D.) of 1 μM. The sensitivity of this amperometric biosensor could be increased up to a factor of five when the hydrogel was blended with SWCNTs of different lengths. Different fractions of SWCNTs were analyzed with TEM in order to characterize the SWCNTs and trace additional impurities. The sensitivity-increasing effect of the SWCNTs strongly depended on their purity and their average length. This effect was clearly caused by the nanotubes, not by the transition metal particles, which were present to some extent. In our assembly we detected the largest increase when SWCNTs of medium length were applied. The increase in current seems not to be caused by a partial unfolding of the enzyme because this process is expected to be most effective with the shortest fraction of SWCNTs. We propose that the sensitivity-increasing effect is caused mainly by the structural and electrical properties of the SWCNTs. There exists an optimum length for the SWCNTs, which allowed an efficient blending and a charge transport over large distances at the same time. For different types of redox enzymes the optimum length of the SWCNTs varies and has to be optimized for each individual case.

The NADH sensitive amperometric biosensor developed in this work exhibited excellent performance and the electrocatalytic system consisting of DI embedded in an osmium redox polymer hydrogel blended with SWCNTs can be extended with NAD^+-dependent dehydrogenases, which catalyze the oxidation of specific substrates with concomitant NAD^+-reduction (Antiochia and Gorton, 2007). Thereby a large number of amperometric biosensors based on NADH redox cycling can be realized.

Acknowledgements

This work was supported by the Deutsche Forschungsgemeinschaft DFG (DFG postdoc fellowship NO 740/1-1) and the Swedish Research Council.

References

Antiochia, R., Gorton, L., 2007. Biosens. Bioelectron. 22, 2611–2617.
Appelqvist, R., Marko-Varga, G., Gorton, L., Torstensson, A., Johansson, G., 1985. Anal. Chim. Acta 169, 237–247.
Balavoine, F., Schultz, P., Richard, C., Mallouh, V., Ebbesen, T.W., Mioskowski, C., 1999. Angew. Chem. Int. Ed. 38, 1912–1915.
Banks, C.E., Crossley, A., Salter, C., Wilkins, S.J., Compton, R.G., 2006. Angew. Chem. Int. Ed. 45, 2533–2537.
Bardea, A., Katz, E., Bückmann, A.F., Willner, I., 1997. J. Am. Chem. Soc. 119, 9114–9119.
Barton, S.C., Gallaway, J., Atanassov, P., 2004. Chem. Rev. 104, 4867–4886.
Binyamin, G., Cole, J., Heller, A., 2000. J. Electrochem. Soc. 147, 2780–2783.
Britz, D.A., Khlobystov, A.N., 2006. Chem. Soc. Rev. 35, 637–659.
Bullen, R.A., Arnot, T.C., Lakeman, J.B., Walsh, F.C., 2006. Biosens. Bioelectron. 21, 2015–2045.
Callegari, A., Cosnier, S., Marcaccio, M., Paolucci, D., Paolucci, F., Georgakilas, V., Tagmatarchis, N., Vazquez, E., Prato, M., 2004. J. Mater. Chem. 14, 807–810.
Choi, H.N., Lyu, Y.-K., Han, J.H., Lee, W.-Y., 2007. Electroanalysis 19, 1524–1530.
De Leo, M., Kuhn, A., Ugo, P., 2007. Electroanalysis 19, 227–236.
Ericson, L.M., Fan, H., Peng, H., Davis, V.A., Zhou, W., Sulpizio, J., Wang, Y., Booker, R., Vavro, J., Guthy, C., et al., 2004. Science, 305, 1447–1450.
Fagan, J.A., Simpson, J.R., Bauer, B.J., De Paoli Lacerda, S.H., Becker, M.L., Chun, J., Migler, K.B., Hight Walker, A.R., Hobbie, E.K., 2007. J. Am. Chem. Soc. 129, 10607–10612.
Forrest, G.A., Alexander, A.J., 2007. J. Phys. Chem. C 111, 10792–10798.
Gooding, J.J., Shapter, J.G., 2005. Methods Mol. Biol. 300, 225–241.
Gorton, L. Domínguez, E., Encyclopedia of Electrochemistry, (Series Eds. A. J. Bard, M. Stratmann), Vol. 9 (Ed. G. S. Wilson), Bioelectrochemistry, Wiley-VCH, Weinheim, 2002, pp. 67–143.
Granot, E., Basnar, B., Cheglakov, Z., Katz, E., Willner, I., 2006. Electroanalysis 18, 26–34.
Heller, A., 2004. Phys. Chem. Chem. Phys. 6, 209–216.
Iijima, S., 1991. Nature 354, 56–58.
Joshi, P.P., Merchant, S.A., Wang, Y., Schmidtke, D.W., 2005. Anal. Chem. 77, 3183–3188.
Lawrence, N.S., Deo, R.P., Wang, J., 2005. Electroanalysis 17, 65–72.
Lee, Y.-J., Lyu, Y.-K., Choi, H.N., Lee, W.-Y., 2007. Electroanalysis 19, 1048–1054.
Li, J., Qiu, J.-D., Xu, J.-J., Chen, H.-Y., Xia, X.-H., 2007. Adv. Funct. Mater. 17, 1574–1580.
Liu, A.-R., Wakayama, T., Nakamura, C., Miyake, J., Zorin, N.A., Qian, D.-J., 2007. Electrochim. Acta 52, 3222–3228.
Liu, J., Chou, A., Rahmat, W., Paddon-Row, M.N., Gooding, J.J., 2005. Electroanalysis 17, 38–46.
Liu, J., Paddon-Row, M.N., Gooding, J.J., 2004. J. Phys. Chem. B 108, 8460–8466.
Liu, S., Cai, C., 2007. J. Electroanal. Chem. 602, 103–114.
Luo, X., Killard, A.J., Smyth, M.R., 2006. Electroanalysis 18, 1131–1134.
Ma, Y., Ali, S.R., Dodoo, A.S., He, H., 2006. J. Phys. Chem. B 110, 16359–16365.
Mains, I., Power, D.M., Thomas, E.W., Buswell, J.A., 1980. Biochem. J. 191, 457–465.
Mano, N., Kuhn, A., 2001. Biosens. Bioelectron. 16, 653–660.
Mano, N., Thienpont, A., Kuhn, A., 2001. Electrochem. Commun. 3, 585–589.
Mao, F., Mano, N., Heller, A., 2003. J. Am. Chem. Soc. 125, 4951–4957.
Messersmith, P.B., Textor, M., 2007. Nat. Nanotechnol. 2, 138–139.
Musameh, M., Wang, J., Merkoci, A., Lin, Y., 2002. Electrochem. Commun. 4, 743–746.
O'Connor, M., Kim, S.N., Killard, A.J., Forster, R.J., Smyth, M.R., Papadimitrakopoulos, F., Rusling, J.F., 2004. Analyst 129, 1176–1180.

Ohara, T.J., Rajagopalan, R., Heller, A., 1993. Anal. Chem. 65, 3512–3517.
Patolsky, F., Weizmann, Y., Willner, I., 2004. Angew. Chem. Int. Ed. 43, 2113–2117.
Rivas, G.A., Rubianes, M.D., Pedano, M.L., Ferreyra, N.F., Luque, G.L., Rodríguez, M.C., Miscoria, S.A., 2007. Electroanalysis 19, 823–831.
Rubianes, M.D., Rivas, G.A., 2005. Electroanalysis 17, 73–78.
Ruzicka, J., Hansen, E.H., 1988. In: Winefordner (Ed.), Flow Injection Analysis, 2nd ed. John Wiley & Sons, New York, pp. 23–26.
Sljukic, B., Banks, C.E., Compton, R.G., 2006. Nano Lett. 6, 1556–1558.
Tasca, F., Timur, S., Ludwig, R., Haltrich, D., Volc, J., Antiochia, R., Gorton, L., 2007. Electroanalysis 19, 294–302.
Timur, S., Anik, U., Odaci, D., Gorton, L., 2007. Electrochem. Commun. 9, 1810–1815.
Tu, X., Xie, Q., Huang, Z., Yang, Q., Yao, S., 2007. Electroanalysis 19, 1815–1821.
Tu, Y., Lin, Y., Yantasee, W., Ren, Z., 2005. Electroanalysis 17, 79–84.
Valentini, F., Orlanducci, S., Terranova, M.L., Amine, A., Palleschi, G., 2004. Sens. Actuators B 100, 117–125.
Wang, J., 2005. Electroanalysis 17, 7–14.
Wang, J., Musameh, M., Lin, Y., 2003. J. Am. Chem. Soc. 125, 2408–2409.
Wang, Y., Joshi, P.P., Hobbs, K.L., Johnson, M.B., Schmidtke, D.W., 2006. Langmuir 22, 9776–9783.
Xue, H.G., Sun, W.L., He, B.J., Shen, Z.Q., 2002. Chin. Chem. Lett. 13, 799–800.
Zhang, Y., Pan, Y., Su, S., Zhang, L., Li, S., Shao, M., 2007. Electroanalysis 19, 1695–1701.
Zhao, Y.-D., Zhang, W.-D., Chen, H., Luo, Q.-M., 2002. Anal. Sci. 18, 939–941.
Ziegler, K.J., 2005. Trends Biotechnol. 23, 440–444.